An integrated epigenome and transcriptome analysis identifies PAX2 as a master regulator of drug resistance in high grade pancreatic ductal adenocarcinoma

Imlimaong Aier[1], Rahul Semwal[2], Aiindrila Dhara[3], Nirmalya Sen[3,4]*, Pritish Kumar Varadwaj[1]*

1 Department of Bioinformatics & Applied Sciences, Indian Institute of Information Technology—Allahabad, Uttar Pradesh, India, **2** Department of Information Technology, Indian Institute of Information Technology—Allahabad, Uttar Pradesh, India, **3** Cancer Research Program, Rajiv Gandhi Centre for Biotechnology, Trivandrum, Kerala, India, **4** S.N.Bose Innovation Centre, University Of Kalyani, Nadia, West Bengal, India

* pritish@iiita.ac.in (PKV); nirmalya@rgcb.res.in, nirmalyarffs19@klyuniv.ac.in (NS)

Abstract

Pancreatic ductal adenocarcinoma (PDAC) is notoriously difficult to treat due to its aggressive, ever resilient nature. A major drawback lies in its tumor grade; a phenomenon observed across various carcinomas, where highly differentiated and undifferentiated tumor grades, termed as low and high grade respectively, are found in the same tumor. One eminent problem due to such heterogeneity is drug resistance in PDAC. This has been implicated to ABC transporter family of proteins that are upregulated in PDAC patients. However, the regulation of these transporters with respect to tumor grade in PDAC is not well understood. To combat these issues, a study was designed to identify novel genes that might regulate drug resistance phenotype and be used as targets. By integrating epigenome with transcriptome data, several genes were identified based around high grade PDAC. Further analysis indicated oncogenic PAX2 transcription factor as a novel regulator of drug resistance in high grade PDAC cell lines. It was observed that silencing of PAX2 resulted in increased susceptibility of high grade PDAC cells to various chemotherapeutic drugs. Mechanistically, the study showed that PAX2 protein can bind and alter transcriptionally; expression of many ABC transporter genes in high grade PDAC cell lines. Overall, the study indicated that PAX2 significantly upregulated ABC family of genes resulting in drug resistance and poor survival in PDAC.

Introduction

Pancreatic cancer is the fourth leading cause of cancer related death in several countries and will surpass breast, prostate cancer to become the second leading cause of cancer related death in the near future [1], [2], [3]. With no apparent symptoms in its early stages, pancreatic cancer grows aggressively, infiltrating adjacent tissues and promoting metastasis along with resistance to chemo and radiotherapy [4], [5]. Most of the patients are present with metastatic disease or

local infiltration at the time of initial diagnosis, and only 15–20% of the patients are candidates for surgical resection. Out of the several types of pancreatic cancer, pancreatic ductal adeno-carcinoma (PDAC) is the most common (85%) [6].

Clinically, histological alterations indicating more differentiated PDACs are termed as low grade, while the undifferentiated tumors are termed as high grade PDAC [7], [8]. The clinical aspects that might help PDACs develop drug resistance includes tumor heterogeneity, epithelial mesenchymal transition, and upregulated drug transporters [9], [10], [11]. Many ABC family of transporters, like *ABCC1*, *ABCC2*, *ABCC3*, and *ABCC5* have been shown to be upregulated in pancreatic cancer patients [12], [13], [14], [15], [16], [17], [18]. Several studies have established the relationship between ABC family transporter proteins and drug resistance in pancreatic cancer. *ABCC5* expression, for instance, was found to be significantly correlated with cellular sensitivity to 5-fluorouracil (5-FU) [14] and gemcitabine [18], where acquired resistance to 5-FU was associated with an increase in *ABCC5* expression [14]. Further, it was reported that expression levels of *ABCC3* and *ABCC5* changed during tumor development, and the expression of *ABCC3* was significantly correlated with high tumor grade. It was also observed that *ABCC3* expression was linked to survival in patients, where patients with lower expression of the gene had longer survival period [12]. Upregulation of *ABCC2* and *ABCC1* is often expressed in a PDAC cohort [19]. *ABCC2* is correlated with negative prognosis in several forms of carcinomas, while *ABCC1* expression reportedly increased when exposed to high doses of gemcitabine in PDAC [20]. However, a distinct regulation of these transporters with respect to tumor grade is not well understood.

To understand the underlying mechanism of PDAC behavior due to its heterogeneity, an integrative study was conducted to identify enriched regions within the genome marked by histone methylation regulators, and to correctly assign the upregulation and downregulation of important genes present within these regions. In addition, network study to understand the underlying biological process and pathway of significantly enriched genes present in the high grade cell lines were conducted. Oncogenic transcription factor PAX2 (belonging to the conserved DNA-binding paired box domain family) showed strong physical network in PDAC cell lines belonging to high grade tumors. Additionally, it was found that PAX2 silencing in pancreatic cancer cells increases susceptibility towards known clinical agents. Our study reveals that PAX2 transcriptionally regulates the expression of several drug transporter family members like *ABCC1*, *ABCC2*, *ABCC3*, and *ABCC5* by binding to the promoters of these drug resistance genes. Overall, this study establishes data integration and mining methods to identify and mechanistically validate genes regulating high grade PDAC related oncogenesis.

Materials and methods

Data retrieval, quality check and sequence alignment

The data for the analysis were obtained from NCBI GEO database, deposited by Nicoli P et al [8]. Details about the cell lines used for the study are given below (Table 1):

Quality check on the raw data files were done using FastQC (http://www.bioinformatics.babraham.ac.uk/projects/fastqc), a tool for assessing the quality of NGS data. For RNA-Seq data, HISAT2 [21] was used for alignment of sequences due to its speed and sensitivity. Forward and reverse strands of each replicates were aligned using built-in genome for reference (hg19). The mean distance between pairs was set to 200bp for each sample.

Read count and Expression analysis

FeatureCounts [22], a highly optimized read counting tool was used for the study because of its speed and reliability. Aligned RNA-Seq reads in the form of Binary Alignment Map (BAM) was provided as input, along with a list of genomic features in Gene Transfer Format (GTF)

Table 1. ChIP-Seq and RNA-Seq datasets with corresponding ID.

	Cell-line	GEO ID			
		ChIP-Seq		RNA-Seq	
		H3K4Me1	H3K4Me3	Replicate 1	Replicate 2
Low grade PDAC	Control	GSM1574271			
	CAPAN-2	GSM1574243	GSM1574258	GSM1574299	GSM1574300
	CFPAC-1	GSM1574245	GSM1574259	GSM1574301	GSM1574302
High grade PDAC	Control	GSM1574272			
	MIA PaCa-2	GSM1574250	GSM1574261	GSM1574305	GSM1574306
	PANC-1	GSM1574252	GSM1574262	GSM1574307	GSM1574308

https://doi.org/10.1371/journal.pone.0223554.t001

for human reference genome Human GRCh37 (hg19). The procedure was carried out for all the replicates. DeSeq2 [23], a package in R for differential gene expression, was used for this study. The dataset were divided into low grade group, consisting of CAPAN-2 and CFPAC-1 replicates, and high grade group, consisting of MIA PaCa-2 and PANC-1 replicates. Differential gene expression analysis was performed by considering the low grade group as control, and the high grade ones as treatment.

ChIP-Seq data for PDAC were aligned using Bowtie2 [24], a fast memory efficient tool for large sequence alignment. All reads were single-end, and were mapped using built-in genome index with hg19 as the reference genome. The computational analysis of ChIP-Seq experiment started with fastq files containing an associated per-nucleotide quality score Q that is an estimation of the -10*log (p), where p is the probability that the corresponding base call is incorrect. The pipeline involves quality assessment by plotting base qualities and frequencies per sequencing cycle, alignment to the genome, duplicate filtering of alignments, removal of low complexity regions and transformation of the aligned data to coverage vectors.

Peak calling and peak correlation

MACS2 [25] is a program that is widely considered the best tool for ChIP peak identification. It makes use of a parametric model based on a local Poisson distribution parameterized from the control data. The filtered and aligned dataset obtained from the previous step was then provided as input for peak calling and identification. The enriched regions for H3K4Me1 and H3K4Me3 were discovered using default settings with BW = 300, along with the broad peaks option. The comparison for each sample was made with its corresponding input data.

Correlation between the peaks of all datasets were compared using deep sequencing tools [26] present in the Galaxy platform [27] for visualization of deeply sequenced data. BAM files generated by Bowtie2 were processed using the module bamCoverage to reduce the size of data. This resultant data was saved in bigwig format. The data was then compared against each other based on their difference using the module bigwigCompare. Correlation plot of all the datasets were then computed using Spearman correlation coefficients. EaSeq [28], a tool for ChIP-Seq data analysis and visualization was used for annotation of genes to peak regions, and the peak intensity of low grade and high grade PDAC peaks were compared. Visualization of peak regions around genes were carried out using UCSC browser [29].

Integrative analysis of ChIP and RNA-Seq data using BETA, Gene Ontology and network analysis

Binding and Expression Target Analysis (BETA) [30] is an integrative tool for the analysis of transcription factors and chromatin regulator binding sites from ChIP-Seq by correlating with

differentially expressed genes from RNA-Seq. The main purpose of this tool is to determine the activating and repressing function of each gene, which is detected using a nonparametric statistical test.

For this study, BETA was used for the integration of ChIP with RNA-Seq. Peak files of each cell line were correlated with their corresponding differentially expressed gene data according to their methylation state. The operation was carried out using hg19 as the reference genome, and by setting the Benjamini-Hochberg false discovery rate (FDR) for differentially expressed genes at ≤ 0.05. The result from this analysis consisted of a list of upregulated and down regulated genes along with their ranks based on the regulatory potential of factor binding and differential expression upon factor binding.

Enrichment analysis of high-throughput data was calculated inclusive of parameters like Chi-square, Fisher's exact test, Binomial probability and Hypergeometric distribution [31]. The genes identified from high-throughput screening are then annotated with Gene Ontology (GO) [32] terms. Cytoscape [33], an open source tool for visualization and analysis of complex networks, was used for the analysis of expressed gene data network. Cytoscape gives the ability to integrate arbitrary data on the graph, while serving as a platform for its visual representation. Moreover, the interface has the means to implement external methods in the form of plug-ins. Biological Networks Gene Ontology tool (BinGO) [34], a plugin for ontology analysis in Cytoscape, was used for ontological analysis of biological processes, and the connections between selected genes were studied using GeneMANIA [35], a tool for generating hypothesis on gene function and analysis of gene sets. For BinGO, overrepresented genes were specified for the visualization, which were selected using a hypergeometric test, with an FDR of 0.05. GO biological process was selected as the preferred ontology process for *Homo sapiens*, exclusively. GeneMANIA parameters were specifically restricted to genetic interactions, physical interactions, and shared pathways, to further isolate and study relevant connections between selected genes. All weightage provided were set to automatic. Comparison between the upregulated and downregulated genes of high grade data, and analysis of key genes were visualised in the form of a Venn diagram using the tool FunRich [36], an enrichment tool which provides graphical output for data visualization. FunRich was also used for assigning ontology process to a few selected genes from UniProt database [37] for an FDR of ≤ 0.05. Pathway analysis was conducted using ClueGo [38] by selecting KEGG pathways for the desired ontology. Genes that occur below a threshold of p-value ≤ 0.05 were investigated at global level network specificity. Pathways relevant to cancer were investigated using Pathview [39], with the help of individual cell line gene expression data from DEGUST (http://degust.erc.monash.edu/) using edgeR [40]. HGPEC [41], a plugin for Cytoscape which uses a random walk with restart on heterogeneous data (RWRH) algorithm, was used to predict the disease-gene association on heterogeneous network. In this method, a list of known genes from given diseases are used as training data. A complete different set of genes, which do not appear on the training set of genes, serve as the candidate gene set. The RWRH algorithm then uses the training data to identify and classify all candidate genes and disease in the heterogeneous network.

Cell culture, reagents and transfection

MIA PaCa-2 (MIA PaCa-2 ATCC® CRL-1420™) cells and PANC-1 (PANC-1 ATCC® CRL-1469™) cells were provided by Dr. Hari Kumar KB (RGCB, India). Both cells were cultured in DMEM medium, (Thermo Fisher Scientific, Waltham, MA), supplemented with 10% fetal bovine serum (FBS), at 37˚C, 5% CO2. The identity of cell lines were confirmed by STR (Short Tandem Repeats) profiling using standard primer sets for core human loci (https://strbase.nist.gov/coreSTRs.htm) and the cells were determined to be mycoplasma free using MycoAlert

Mycoplasma detection kit from Lonza (NJ, USA). For RNAi studies, previously validated PAX2 siRNA (5'CATCAGAGCACATCAAATC3', [42]) (Integrated DNA Technologies, Inc., USA) was used and cells were transfected using 20 nM siRNA complexed with RNAi-Max (Thermo Fisher Scientific).

The siCell Death, siRNA used as Positive cell death phenotype control, from qiagen, USA. This commercially available siRNA known as AllStars Hs Cell Death siRNA (Catalogue Number SI04381048). Camtothecin and 5'Flurouracil were purchased from Tocris biosciences and dissolved according to instructions. Gemcitabine was purchased from Santa Cruz biotechnology and dissolved as per instructions.

mRNA analysis

For real-time PCR analysis, total RNA from cells was extracted using RNA extraction kit (Thermo Fisher Scientific, MA), and cDNA was synthesized using the iScript cDNA synthesis kit (Bio-Rad, Hercules, CA) following the manufacturer's protocol. For normalization 18S ribosomal RNA was used as a reference. The following primer sets were used for SYBR green based qPCR: PAX2: `Forward primer 5'- CAACGGTGAGAAGAGGAAACGAG -3'`, `Reverse Primer 5'- TAATGCTGCTGGGTGAAGGTGTC-3'` [43], 18sRNA: `Forward 5'- GTAACCCGTTGAACCCCATT-3'`, `Reverse 5'- CCATCCAATCGGTAGTAGCG 3'`, ABCC2/MRP2: `Forward 5'- ACGGGCACATCACCATCAAG -3'`, `Reverse 5'- CTCCAGGCAGCATTTCCAAG -3'` [44], ABCC3/MRP3: `Forward 5'- CGCCTGTTTTTCTGGTGGTT -3'`, `Reverse 5'- TTGTGTCGTGCCGTCTGCTT -3'` [44], ABCC1/MRP1: `Forward 5'- ACCCTAATCCCTGCCCAGAG -3'`, `Reverse 5'- CGCATTCCTTCTTCCAGTTC -3'` [44], ABCC5/MRP5: `Forward 5'- CCAAGCTGACCCCCAAAATGAAAAA -3'`, `Reverse 5'- TGGATGTGCTTGCCTTCTTCCTCTTC -3'` [44], TM4SF1: `Forward 5'- AAGGGGGAGAAAACCTAGCA -3'`, `Reverse 5'- CCAGCCCAATGAAGACAAAT -3'` [45].

Chromatin Immunoprecipitation assays

ConTra V3 [46] was used for the identification of TFBS across the promoter regions of ABC transporter family of genes, which was further verified using the GTRD [47]. This process was carried out to find conserved regions of PAX2 protein, and to extract these features for the designing of primers. Chromatin immunoprecipitations were carried out using a kit following the manufacturer's protocol (Millipore). Briefly, 1×10^7 cells were fixed with formaldehyde and lysed with SDS Lysis Buffer. The cell lysates were then sonicated to shear the DNA to lengths between 0.2-1kb. The samples were precleared with Protein agarose slurry. Control normal Rabbit IgG (Catalogue No#2729, Cell Signalling Technology, USA) or Anti-PAX2 Rabbit (Catalogue No# ab23799, AbCam Plc, UK) antibody was added (concentration 10μg/ml) and incubated overnight at 4°C followed by incubation with fresh Protein agarose slurry for 2 hours. Precipitated chromatin complexes were removed from the beads through 30-min incubation with 500 μL of elution buffer. Finally, the protein–DNA cross-links were reversed by incubation at 65°C for 4 hours and immunoprecipitated DNA was analyzed by qPCR. Primers used for this analysis are given below:

`ABCC2: 5'GGACCACTCTGCTTATCTTGGA3'; 5'GGTGTGCTGCAGTGTAAATCA 3'`
`ABCC5: 5' GATAATCAGCTAAGCTAGGGAAC3'; 5'CCATAAAGAACAGCGGCTCAC3'`
`ABCC1: 5'GGTGTCTCTCTGCTTCTGT3'; 5'CTTTCTACAATCTAAGCCCC3'`
`ABCC3: 5' ATGAAGGCAGAGCTGGGATA3'; 5' GTGCGATCATAGCTCACAGTA3'`

TM4SF1: 5' CCAGGCTGGTCTTGAACTCAT3'; 5'CGAAAGAAACTTAAGTGTGAT
G3'

Cell viability and caspase assay

Caspase activation and cell viability was measured using the CaspaseGlo 3/7 and the CellTiter-GloⓇ Luminescent assay systems respectively (Promega) as per manufacturer's instruction using at least three biological replicas of each treatment. Spark10M luminometer from Tekan was used for luminescence measurement.

Statistical analysis

Statistically significant differentially expressed genes and BETA analysis were identified using Benjamini-Hochberg false discovery rate. Enriched ChIP-Seq peaks were identified using empirical false discovery rate. For gene ontology studies, hypergeometric test and Benjamini-Hochberg false discovery rate were performed. Statistical analysis was performed for all wet lab experiments. Experiments were performed as biological triplicates. Dunnette's multiple comparison test, Student t-test were performed for cell survival data. For real time PCR data, SEM ±3 of biological triplicates were considered. All data were found to be statistically significant.

Results and discussion

Analysis of PDAC dataset

The quality of dataset used for analysis of PDACs were verified using FastQC and the mean quality scores of all cell lines indicated that the data lies in the good quality call region with minimal chances of error. The total number of expressed genes obtained were 20,795, out of which the number of genes classified as differentially expressed were 1044 over-expressed and 2092 under-expressed genes based on an FDR of 0.05 (5%) and fold enrichment > 2. Fig for correlation between the samples, and the volcano plot for differentially expressed genes were provided (S1 Fig), while a comprehensive list of all up/downregulated genes can be found in S1 Table. Genes below this particular threshold were discarded from further use.

PDAC dataset was analyzed for activating methylation signatures (Monomethylation; H3K4Me1 vs. Trimethylation; H3K4Me3) in MIA PaCa-2 and PANC-1 cells belonging to the high grade PDAC cell lines (Fig 1). Low grade PDAC cell lines represented by CFPAC-1 and CAPAN-2 were also used as controls during data analysis.

During signal intensity comparison between methylated peaks (Fig 1A), the monomethylated peaks for low grade lines (CAPAN-2 and CFPAC-1), displayed a deep shade of blue, corresponding to greater correlation. In the case of trimethylated peaks for low grade samples, correlation between CAPAN-2 and CFPAC-1 became distant, with CAPAN-2 H3K4Me3 peaks clustering more towards trimethylated peaks representing High grade cell lines (Fig 1B). Monomethylated and trimethylated high grade samples, MIA PaCa-2 and PANC-1, on the other hand, displayed good correlation, indicating close association between the cell lines. High grade PDAC cell line (MIA PaCa-2 and PANC-1) peak frequencies were on par for H3K4Me3, with a high intensity. Although H3K4Me1 peak intensities for MIA PaCa-2 and PANC-1 were on the lower end, very similar peak profiles were observed (Fig 1C). Overall, peak intensity for high grade PDAC were closely matched for all cell lines. On the other hand, low grade PDAC peak intensity for each cell line was varied (Fig 1B). The results from methylation pattern comparison indicated that high grade tumors are more likely to show similar gene expression for methylated promoter regions.
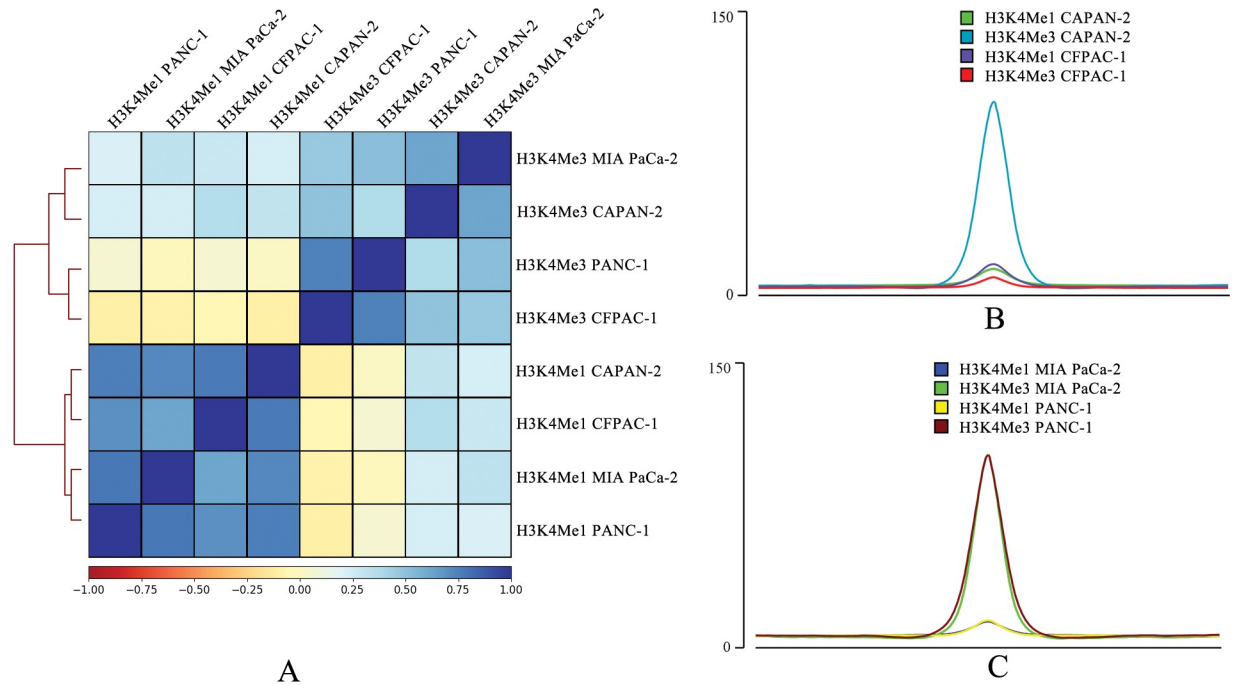
Fig 1. Correlation plot for high grade PDAC ChIP-Seq dataset and peak signal intensity. (A) Spearman correlation plot for low and high grade PDAC ChIP-Seq dataset. Correlation comparison of peak signal intensity for (B) Low grade PDAC cell lines and (C) High grade PDAC cell lines.

To analyze the differentially expressed genes associated with altered methylation in high grade lines, BETA Plus analysis was performed on high grade cell lines by integrating ChIP-Seq data with RNA-Seq data, thus providing a list of upregulated and downregulated genes. Activation and repression function of histone methylation were predicted from PDAC cell lines, and upregulated/downregulated genes were visualized in the form of Venn diagrams (S2 and S3 Figs). Cytoscape and BinGO tools identified a large interconnected cluster, displaying affinity towards cellular differentiation and structure development (Fig 2A), with optimal FDR. This interconnected network was further isolated and the participating gene components, with a strong relation to cancer, were verified through text mining. This group of genes were then analyzed using GeneMANIA to decipher the interconnection between them. The criteria for the interconnection were specifically assigned for co-expression, and physical and genetic interactions. From the generated network (Fig 2B), it was found that *PAX2* gene had the highest number of physical interactions, thus making it an important target. Other genes that were highlighted in the network like *DDR2*, *DPYSL5*, *SPARC*, and *FAM5C* were also evaluated to understand their contribution in the growth and resistance of PDAC. Additional ontology analysis for each of the genes mentioned above were conducted to disseminate their individual roles (S4 Fig).

The network of significant pathways predicted by ClueGo was depicted in Fig 3A, where pathways in cancer was highlighted in a red box. It was observed that a majority of the genes were involved in this pathway, and were interconnected with several other essential processes. To further investigate this set of genes, the tool was rerun, but this time at medium level network specificity for a more detailed insight into the pathways involved in cancer. As expected, the genes that partake in pathways in cancer were seen in pancreatic cancer, as well as transcriptional misregulation in cancer (Fig 3B). To understand the contribution of each gene, the
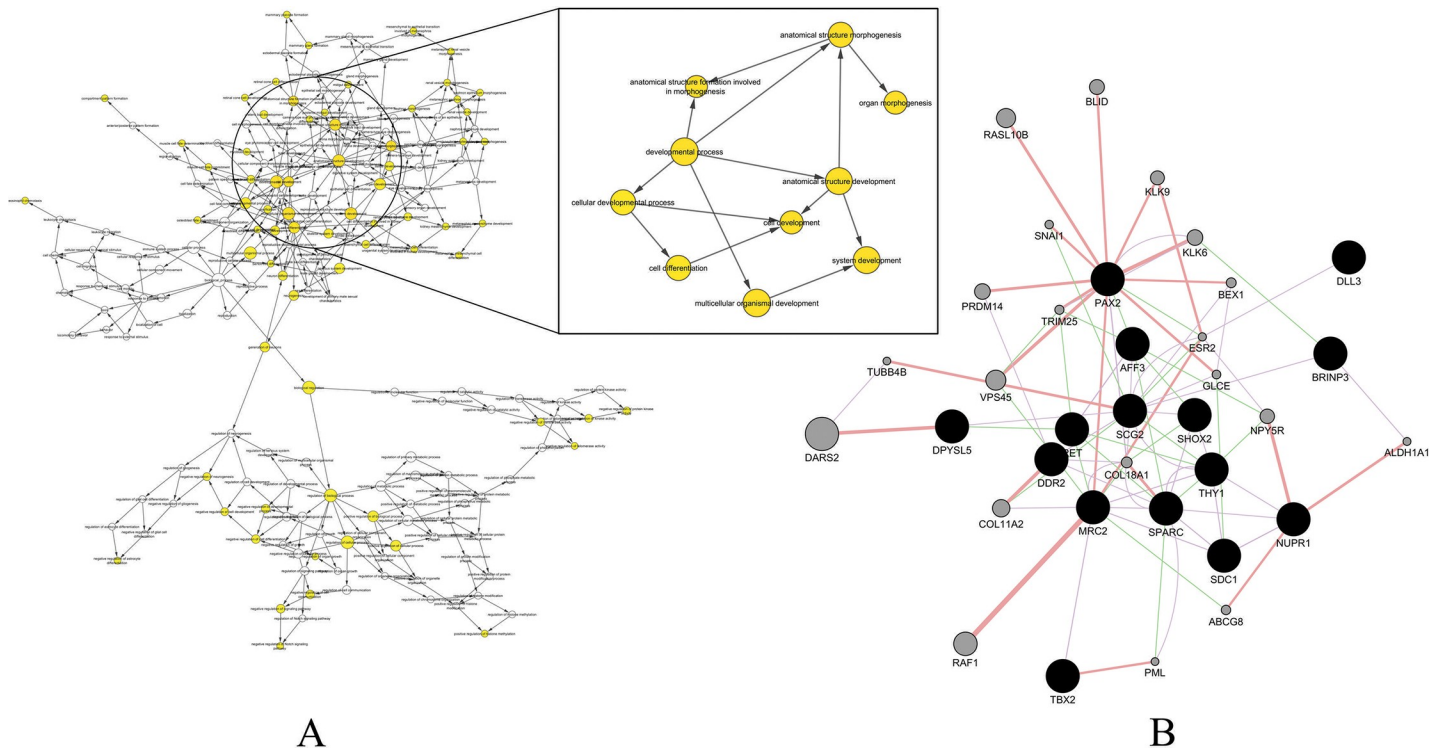
Fig 2. Analysis of high grade PDAC dataset for differential expressed genes using Cytoscape. (A) Representative network cluster for biological process that are actively involved in cell differentiation and structural development were identified using BinGO. Nodes represented in white were not significantly expressed, while a deeper shade of orange correlated with processes predicted with confidence. The inset represents a cluster of biological processes with p-value ≤ 0.05. These clusters were involved in cell differentiation and structural formation. (B) Gene interaction network obtained using GeneMANIA was conducted on selected genes identified from important biological processes. Black nodes represent the selected genes, while grey nodes were automatically drawn by the tool based on their connectivity to the highlighted ones. All edges in the network were derived from prior knowledge.

https://doi.org/10.1371/journal.pone.0223554.g002

fold enrichment for individual cell lines were obtained using DEGUST. Gene expression data from DEGUST output was divided into groups: control (low grade) and sample (high grade), which was then used to generate KEGG pathways for pathways in cancer, transcriptional mis-regulation in cancer and pancreatic cancer using Pathview (S5, S6, and S7 Figs).

The evidence of *PAX2* as an essential gene in the regulation of high grade PDAC was further solidified using HGPEC. Initially, genes from disease closely related to pancreatic cancer were selected from DisGeNET database [48] present in HGPEC. This set of genes were used as training dataset. For the candidate gene set (test dataset), the genes identified from the current study were used as input. This provided us with a comprehensive network of genes predicted to be involved in pancreatic cancer (Fig 4).

To biologically validate our findings, we silenced individual gene like *PAX2, FAM5C, DDR2, DPYSL5,* and *SPARC* in high grade PDAC cell line MIA PaCa-2 using RNAi and accessed cell viability to understand critical function of the genes. We found that mRNA levels of all the genes were downregulated upon RNAi but only *PAX2* downregulation showed consequent decrease in cell viability (~37%) in MIA PaCa-2 cells (S8 Fig).

The octagonal nodes were used to represent candidate genes that were highly ranked in pancreatic cancer. *PAX2* is shown to interact with *RB1*, a prominent tumor suppressor gene [49].
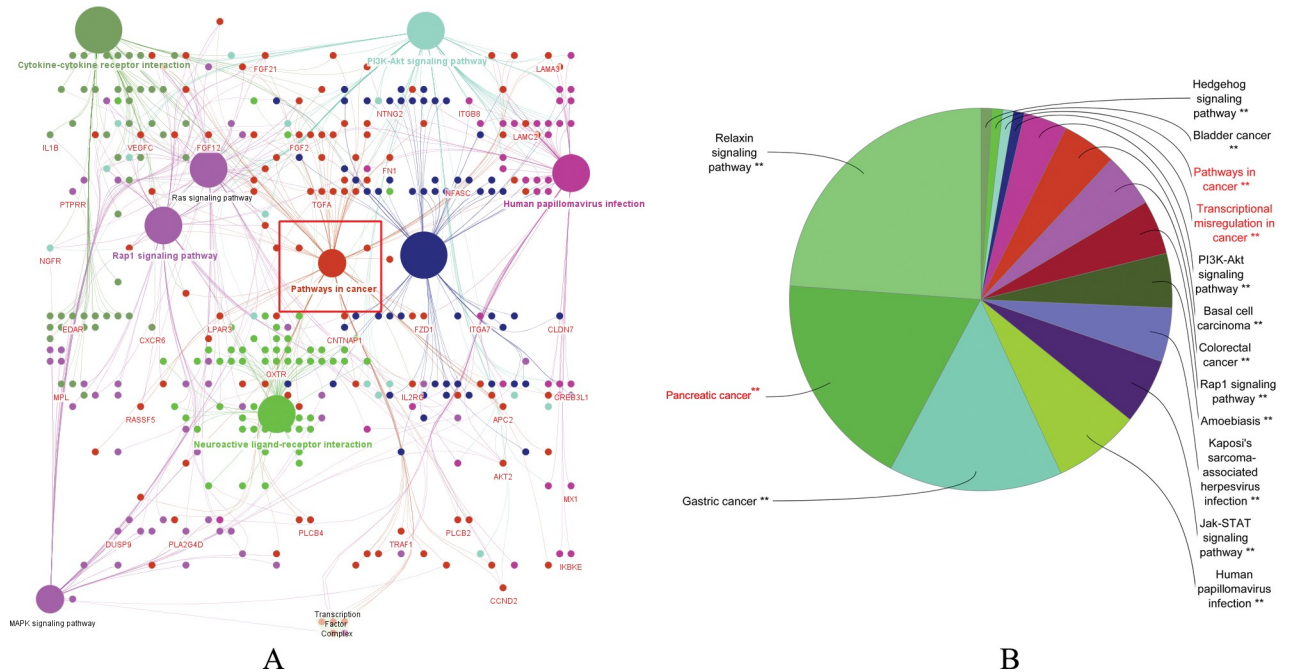
Fig 3. Pathway analysis using ClueGO indicated that several identified genes were interconnected to cancer related pathways. (A) Representation of KEGG pathways enriched in PDAC gene set (Bonferroni step-down corrected p ≤ 0.05). Pathways in cancer (highlighted in a red box) was found to be interconnected to other over-represented terms (B) Pie-chart of pathways expressed in PDAC for gene set extracted from pathways in cancer, with essential pathways marked in red.

PAX2 downregulation increases drug susceptibility in pancreatic cells

PAX2 is known to promote various oncogenic process like metastasis, drug resistance by transcriptionally regulating effector genes in various cancers like Wilms tumor and renal cell carcinoma [50], [51]. Moreover, *PAX2* expression has been linked with EMT transition [52]. However, the role of *PAX2* in high grade PDACs is not known. RNAi based silencing of *PAX2* in high grade PDAC cells (MIA PaCa-2 and PANC-1) resulted in decreased expression of *PAX2* with consequent cell death in MIA PaCa-2 (~37%) and PANC-1 (~34%) cells. Percent cell viability was calculated with respect to Negative control siRNA (siNeg). siCell Death, an siRNA, used as Positive cell death phenotype control (Fig 5A and 5B). Owing to the association of *PAX2* with drug resistance and metastasis in other cancers [53], [54], [55], [56], we were interested to check the effect of *PAX2* silencing with respect to drug treatment in high grade cell lines MIA PaCa-2 and PANC-1 which show more resistance towards drugs like camptothecin, 5' Flurouracil (5'FU), Gemcitabine as reported previously [11], [57], [58], [13], [59], [60], [61], [62], [63], [64]. *PAX2* was silenced followed by addition of Camptothecin or 5'FU (Flurouracil) at varying concentrations in MIA PaCa-2 cells (Fig 5C). Increased cell death (Camptothecin IC_{50} = 0.094 uM, 5'FU IC_{50} = 0.14uM) was observed in cells that were treated with siPAX2 compared to Negative control siRNA transfected MIA PaCa-2 cells (Camptothecin IC_{50} = 6.42 uM, 5'FU IC_{50} = 11.6 uM). Similar increase in drug sensitivity was observed in PANC-1 treated with 5 FU (5'FU IC_{50} = 16.9uM → 0.24uM) upon *PAX2* silencing (Fig 5D). Caspase3/7 activity of these cells were checked under drug treatment and it was found that *PAX2* silenced cells displayed increased caspase3/7 activity compared to control siRNA transfected cells (Fig 5E). Together, these results suggest that *PAX2* might promote drug resistance phenotype in high grade pancreatic cancers.
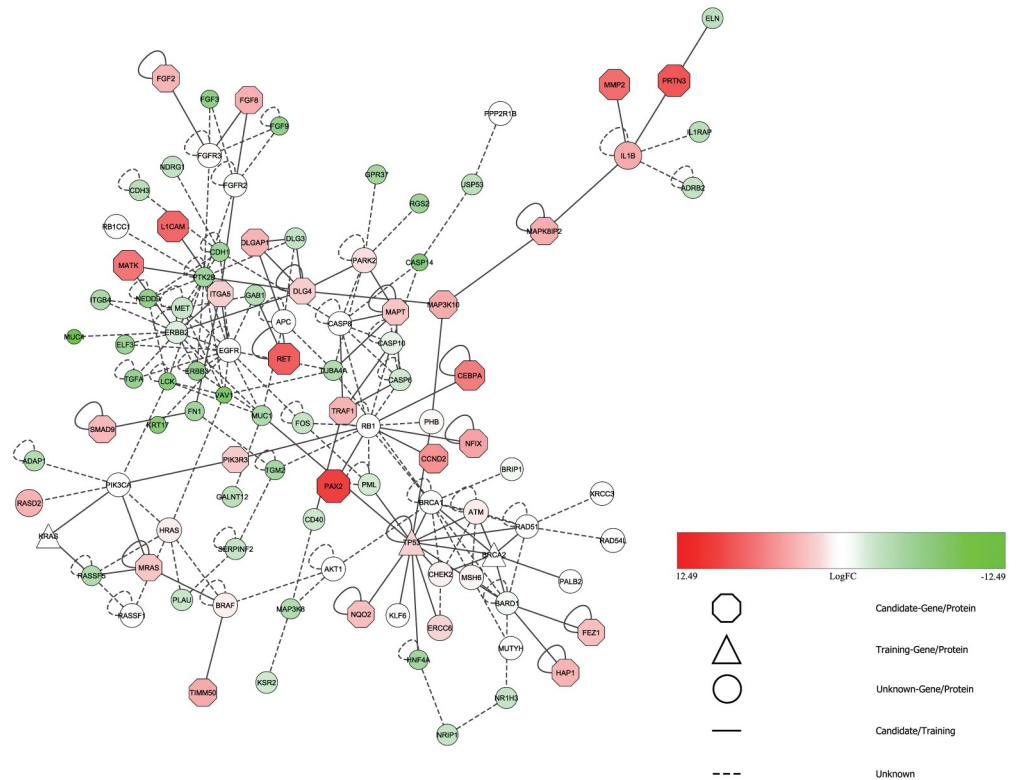
Fig 4. Predicted gene topological relation as obtained from HGPEC.

Gemcitabine in combination with other agents had shown promising effects in PDACs [63], [65]. However, several factors may cooperatively cause gemcitabine resistance which had been associated with aggressiveness and lethality [66], [67], [68], [69]. We checked for *PAX2* involvement during Gemcitabine resistance in high grade PDAC cells. Increasing dose of gemcitabine (upto 160nM) starting from 10nM treatment was used to generate drug resistant MIA PaCa-2 cells (Res-MIA PaCa-2) as described previously [13]. Interestingly, *PAX2* knockdown in Res-MIA PaCa-2 cells was able to decrease cell viability as compared to control siRNA treated cells, thus reestablishing gemcitabine sensitivity (Fig 5F). This data indicated that *PAX2* plays a critical role in development of various drug resistance in PDACs.

PAX2 transcriptionally regulates ABC family of transporters

Various ABC family of transporters are known for promoting drug resistance in pancreatic cancer patients [70], [71]. However, the transcriptional regulation of these transporters in PDACs is not well understood. The expression of *ABCC1*, *ABCC2*, *ABCC3*, *ABCC5* transporters in MIA PaCa-2 cells were studied with respect to *PAX2* knockdown. The expression of *ABCC1*, *ABCC2*, *ABCC3*, *ABCC5* transporters were found to be decreased in *PAX2* silenced cells compared to control siRNA transfected cells (Fig 6A).

We wanted to check if PAX2 transcriptional factor can directly bind and regulate the promoters of the transporter genes. To do this, potential PAX2 binding sites were scanned *in silico* within the promoter regions of ABC transporter family of proteins using ConTra v3. Evidence of binding sites were further confirmed from GTRD. With this information, 200bp sequence in the upstream and downstream region of the TFBS were extracted. The potential binding site for PAX2 in the promoter regions of ABC family transporter proteins are given in S9 Fig.
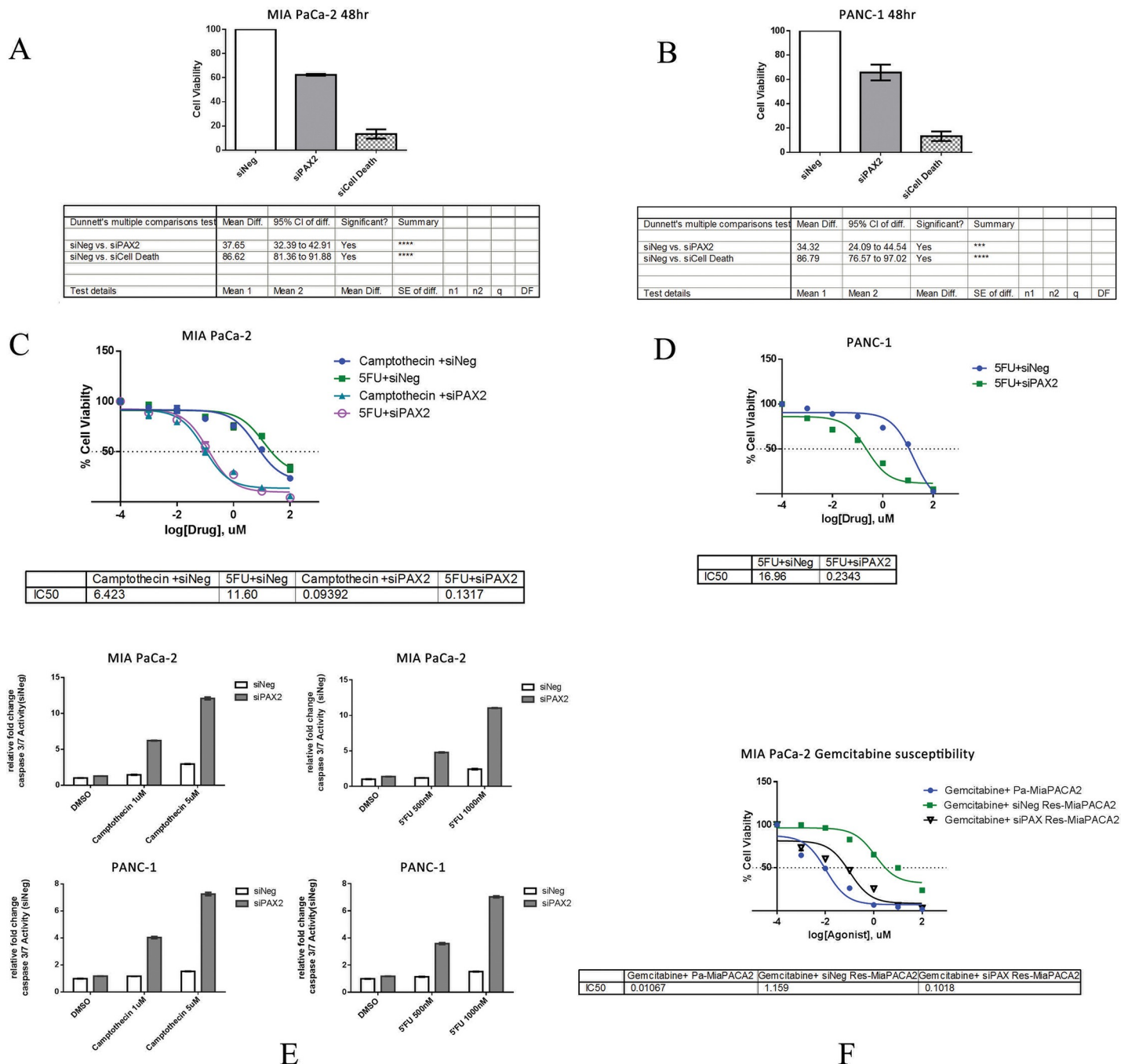
Fig 5. RNAi based silencing of *PAX2* in MIA PaCa-2 and PANC-1 cells led to an increase in drug susceptibility. (A) MIA PaCa-2 and (B) PANC-1 cells were transfected using indicated siRNAs for 48hours. Cell viability assay was performed post 48 hours using luminometer. Percent cell viability was calculated with respect to Negative control siRNA (siNeg). siCell Death, an siRNA used as Positive cell death phenotype control, from qiagen, USA was used as a positive control. Experiments were done independently in triplicates SEM = ± 3. The viability of (C) MIA PaCa-2 and (D) PANC-1 cell lines, previously transfected with siNeg control or siPAX2 siRNA and subsequently (24 hours post transfection) exposed to increasing concentrations of chemotherapeutic drugs camptothecin or 5'Flurouracil for 48 hr (mean ± SEM, n = 3) at each drug concentration normalized to vehicle (V, 0.1% DMSO). (E) Caspase 3/7 activity in MIA PaCa-2 (top panel) or PANC-1 (bottom panel) cell lines, previously transfected with siNeg control or siPAX2 siRNA and subsequently (24 hours post transfection) exposed to indicated concentrations of chemotherapeutic drugs camptothecin or 5'Flurouracil (5'FU) for 48 hours (mean ± SEM, n = 3) at each drug concentration normalized to vehicle (V, 0.1% DMSO). Relative fold change in caspase activity was measured using caspase 3/7 Glo assay using luminometer. (F) The viability of MIA PaCa-2 parental (Pa-MIA PaCa-2) or Gemcitabine resistance MIA PaCa-2 (Res-MIA PaCa-2) cell lines, previously transfected as indicated, with siNeg control or siPAX2 siRNA and subsequently (24 hours post transfection) exposed to increasing concentrations of Gemcitabine for 48 hours (mean ± SEM, n = 3) at each drug concentration normalized to vehicle (V, 0.1% DMSO).
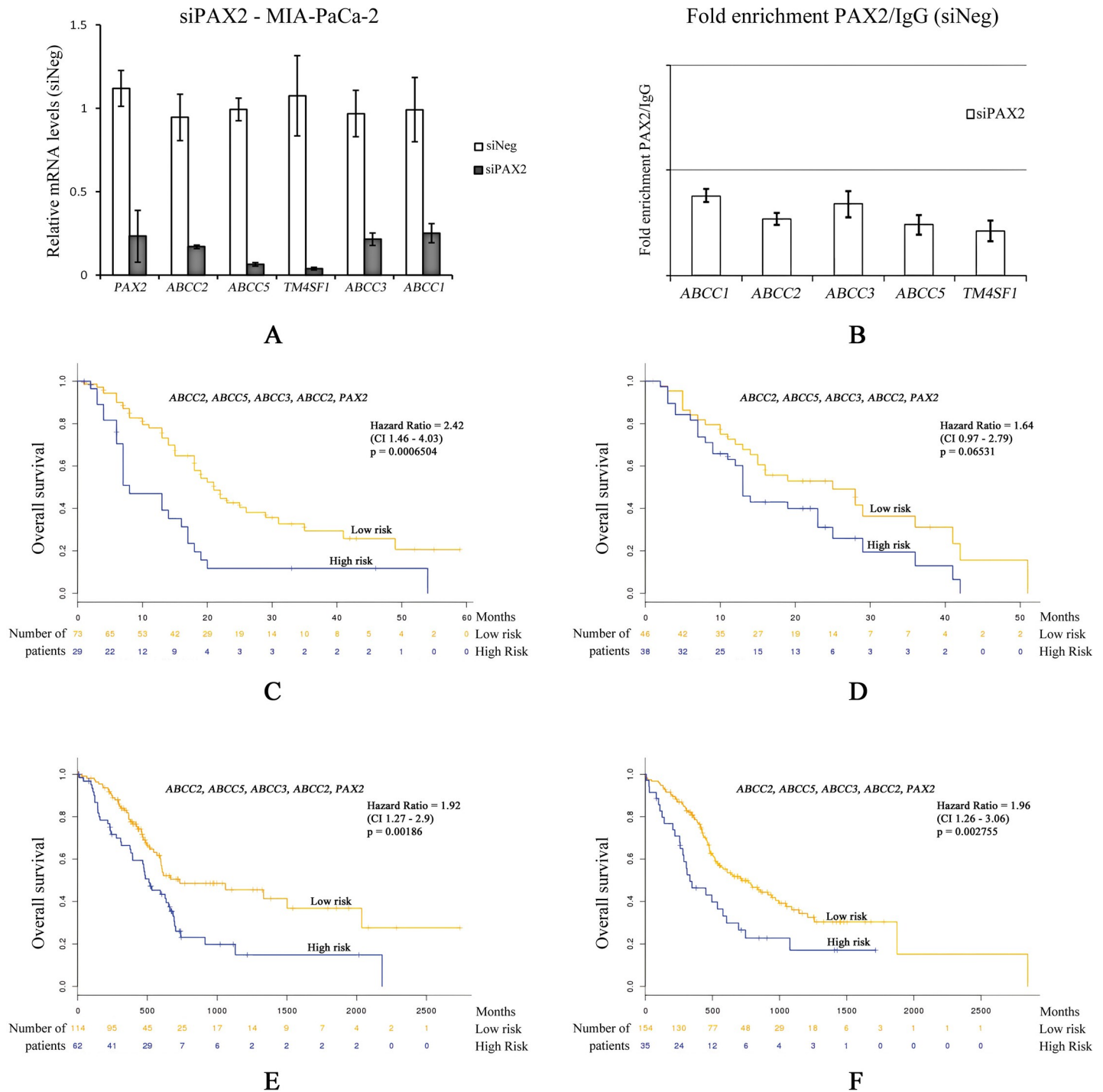
Fig 6. Effect of PAX2 on the transcriptional regulation of *ABC* family of transporters and survival analysis. (A) MIA PaCa-2 cells were transfected with siRNAs against *PAX2*. Relative mRNA levels were analysed with respect to relative mRNA levels (siNEG) 48hours post transfection. Normalization was performed with 18sRNA levels. Experiments were done independently in triplicates SEM = ± 3. (B) MIA PaCa-2 cells were transfected with siNeg or siPAX2 siRNAs. ChIP assay was then performed with *PAX2* antibody or control IgG antibody. The fold enrichment of coprecipitating DNA was determined by qPCR for the indicated promoters. Error bars are means ± SD of three independent experiments with triplicate samples. Survival analysis was performed using Surv Express software [72]. Patient datasets used (C) [73], (D) [74], [75], (E) TCGA pancreatic adenocarcinoma, (F) ICGC portal, for the multivariant analysis of indicated genes *ABCC2*, *ABCC5*, *ABCC3*, *ABCC1* and *PAX2*. High (blue) and low (yellow) represents gene expression.

https://doi.org/10.1371/journal.pone.0223554.g006

Chromatin immunoprecipitation was performed in control siNeg MIA PaCa-2 or siPax2 MIA PaCa-2, using control normal rabbit IgG (Catalogue No#2729, Cell Signalling Technology, USA) or anti-PAX2 rabbit (Catalogue No# ab23799, AbCam Plc, UK) antibody was added (concentration 10μg/ml) and checked for PAX2 promoter occupancy. It was found that PAX2 binds to promoters of *ABCC1*, *ABCC2*, *ABCC3*, *ABCC5* transporters and this binding is decreased upon silencing of *PAX2* in cells. Together these results indicate that PAX2 can be a master regulator of drug resistance in pancreatic cancers by controlling drug transporter cassettes. Inhibitors of PAX2 mediated transcription can be an effective drug target against mixed grade PDAC and can be used to increase susceptibility of end stage PDACs towards existing clinical interventions.

Conclusions

Many previous reports of drug resistance pancreatic cancers indicated the existence of a molecular network that evolves with the progression of PDACs [76], [77], [78], [79], [80]. We speculate that the poorly differentiated mixed grade nature of PDACs harbor the key to such phenotype [81]. Although various factors like *ABC* family of transporters, regulators like *TM4SF1*, various cofactors had been implicated in drug resistance associated with PDACs [82], [83], [18], [13], [14], [84], none of these were able to distinctly classify them to particular tumor grade. Our analysis observed a distinct pattern variation with respect to histone methylation marks and differential gene expression between low grade and high grade PDAC cell types (Fig 1 and S1 Fig). Further analysis of high grade PDAC cells indicated network of genes that show strong physical correlation with tumor progression in selected pathways (Fig 3 and S5, S6, and S7 Figs). PAX2 served as an oncogenic transcription factor in various other cancers by reprogramming gene regulatory networks [85], [86], [87], [54]. Our data shows that PAX2 binds to the promoter region of ABC family genes and regulate their transcription in high grade PDAC cell lines. In addition, it was also found that PAX2 transcriptional factor can bind to the promoter of previously reported transmembrane-domain family *TM4SF1*, a gene that played a role in gemcitabine resistant pancreatic cancer [83]. Silencing *PAX2* expression resulted in down regulation of *TM4SF1* expression, suggesting a possible mechanism for gemcitabine resistance in PDACs (Fig 6A and 6B). Interestingly, our study indicated that the mechanism of *TM4SF1* driven drug resistance might be transcriptionally controlled by PAX2. These findings indicate that PAX2 could act as a master transcription factor regulating drug resistance phenotype in high grade PDACs.

Surprisingly, drug resistance phenotype is a hallmark of lethality associated with PDACs [88], [89], [90]. We found that *PAX2* silencing alone was able to rescue drug susceptibility in high grade cell types with various chemotherapeutic agents (Fig 5). We checked for survival in PDAC patient samples from various available data sets and performed multivariate analysis on *PAX2* and *ABCC* family members. Surprisingly, we found that *PAX2* in combination with *ABCC* transporters were able to significantly alter hazard ratio and survival in PDAC patient (Fig 6C, 6D, 6E & 6F). Together these findings indicate that *PAX2* may have a major prognostic value and future development of *PAX2* inhibitors warrants clinical interventions.

Supporting information

S1 Fig. Correlation plot and volcano plot for high grade PDAC RNA-Seq data. (A) Correlation plot between RNA-Seq data from DESeq2. (B) Volcano plot of upregulated (red) and downregulated (blue) genes in high grade PDAC cell line.
(TIF)

S2 Fig. Activating and repressing function for high grade PDAC cell lines. Activating and repressing function of (A) MIA PaCa-2 H3K4Me1, (B) MIA PaCa-2 H3K4Me3, (C) PANC-1 H3K4Me1 and (D) PANC-1 H3K4Me3. Red lines indicate upregulated genes while the purple line indicates downregulated genes. The black dots represents non-differentially expressed genes (Background). X axis represents the rank of genes based on the regulatory potential while the y axis represents the proportion of genes.
(TIF)

S3 Fig. Overlapping genes in high grade PDAC cell lines. Venn diagram for (A) Common upregulated genes between mono and tri-methylated MIA PaCa-2 and PANC-1 and (B) Common downregulated genes between mono and tri-methylated MIA PaCa-2 and PANC-1. (C) Visualization of enriched peaks around the promoter region of *PAX2* gene indicated that tri-methylation of histones in that region could possibly lead to transcriptional activity of the underlying gene. This was in agreement with the expression data obtained through RNA-Seq analysis.
(TIF)

S4 Fig. Gene Ontology report for biological process, Molecular Function, and Cellular Component of high grade PDAC genes. Gene Ontology report for Biological Process, Molecular Function, and Cellular Component of (A) *DDR2*, (B) *DPYSL5*, (C) *FAM5C*, (D) *PAX2*, and (E) *SPARC* were generated using the FunRich tool. Biological process of *PAX2* presented notable contribution towards negative regulation of apoptosis in general.
(TIF)

S5 Fig. Pathview output for the pathway "Pathways in cancer". Gene components of high grade PDAC were compared against gene components of low grade PDAC, giving rise to the nodes marked in color. Green (-1) depicts genes downregulated in high grade cell line (but upregulated in low grade), while those marked in red (1) depicts upregulated genes in high grade cell line. Some nodes are split between two colors, indicating difference in regulation between MIA PaCa-2 (left) and PANC-1 (right).
(TIF)

S6 Fig. Pathview output for the pathway "Transcriptional misregulation in cancer". Gene components of high grade PDAC were compared against gene components of low grade PDAC, giving rise to the nodes marked in color. Green (-1) depicts genes downregulated in high grade cell line (but upregulated in low grade), while those marked in red (1) depicts upregulated genes in high grade cell line. Some nodes are split between two colors, indicating difference in regulation between MIA PaCa-2 (left) and PANC-1 (right).
(TIF)

S7 Fig. Pathview output for the pathway "Pancreatic cancer". Gene components of high grade PDAC were compared against gene components of low grade PDAC, giving rise to the nodes marked in color. Green (-1) depicts genes downregulated in high grade cell line (but upregulated in low grade), while those marked in red (1) depicts upregulated genes in high grade cell line. Some nodes are split between two colors, indicating difference in regulation between MIA PaCa-2 (left) and PANC-1 (right).
(TIF)

S8 Fig. Relative mRNA levels and cell viability assay for high grade PDAC cell lines. (A) MIA PaCa-2 cells were transfected with siRNAs against indicated genes (Gene of Interest, GOI). Relative mRNA levels were analysed with respect to siRNA Negative control (siNEG) 48hours post transfection. Normalization was performed with 18sRNA levels. Experiments

were done independently in triplicates SEM = ± 3. (B) Mia-Paca2 cells were transfected using indicated siRNAs for 48hours. Cell viability assay was performed post 48 hours using lumin-ometer. Percent cell viability was calculated with respect to Negative control siRNA (siNeg). siCell Death, Death, an siRNA used as Positive cell death phenotype control, from qiagen, USA was used as a positive control. Experiments were done independently in triplicates SEM = ± 3. (C) PANC-1 cells were transfected with PAX2 siRNAs. Relative mRNA levels were ana-lysed with respect to siRNA Negative control (siNEG) 48hours post transfection. Normaliza-tion was performed with 18sRNA levels. Experiments were done independently in triplicates SEM = ± 3.
(TIF)

S9 Fig. Predicted binding site for PAX2 in the promoter regions of ABCC family trans-porter genes. (A) *ABCC1*, (B) *ABCC2*, (C) *ABCC3*, and (D) *ABCC5*.
(TIF)

S1 Table. List of upregulated and downregulated genes found in high grade PDAC cell lines using DeSeq2.
(XLS)

Acknowledgments

Author Contributions

Conceptualization: Imlimaong Aier, Nirmalya Sen, Pritish Kumar Varadwaj.

Data curation: Imlimaong Aier.

Formal analysis: Imlimaong Aier, Rahul Semwal, Aiindrila Dhara.

Funding acquisition: Pritish Kumar Varadwaj.

Investigation: Imlimaong Aier, Rahul Semwal, Aiindrila Dhara, Nirmalya Sen, Pritish Kumar Varadwaj.

Methodology: Imlimaong Aier, Rahul Semwal, Aiindrila Dhara, Nirmalya Sen, Pritish Kumar Varadwaj.

Project administration: Nirmalya Sen, Pritish Kumar Varadwaj.

Resources: Nirmalya Sen, Pritish Kumar Varadwaj.

Software: Rahul Semwal.

Supervision: Nirmalya Sen, Pritish Kumar Varadwaj.

Validation: Aiindrila Dhara, Nirmalya Sen.

Visualization: Imlimaong Aier, Aiindrila Dhara, Nirmalya Sen.

Writing – original draft: Imlimaong Aier, Nirmalya Sen, Pritish Kumar Varadwaj.

Writing – review & editing: Imlimaong Aier, Rahul Semwal, Aiindrila Dhara, Nirmalya Sen, Pritish Kumar Varadwaj.

References

1. Siegel RL, Miller KD, Jemal A. Cancer statistics, 2016. CA: a cancer journal for clinicians. 2016; 66 (1):7–30. https://doi.org/10.3322/caac.21332 PMID: 26742998.

2. Rahib L, Smith BD, Aizenberg R, Rosenzweig AB, Fleshman JM, Matrisian LM. Projecting cancer incidence and deaths to 2030: the unexpected burden of thyroid, liver, and pancreas cancers in the United States. Cancer research. 2014; 74(11):2913–21. https://doi.org/10.1158/0008-5472.CAN-14-0155 PMID: 24840647.

3. Aier I, Semwal R, Sharma A, Varadwaj PK. A systematic assessment of statistics, risk factors, and underlying features involved in pancreatic cancer. Cancer epidemiology. 2019; 58:104–10. https://doi.org/10.1016/j.canep.2018.12.001 PMID: 30537645.

4. Du Z, Qin R, Wei C, Wang M, Shi C, Tian R, et al. Pancreatic cancer cells resistant to chemoradiotherapy rich in "stem-cell-like" tumor cells. Digestive diseases and sciences. 2011; 56(3):741–50. https://doi.org/10.1007/s10620-010-1340-0 PMID: 20683663.

5. Li D, Xie K, Wolff R, Abbruzzese JL. Pancreatic cancer. Lancet. 2004; 363(9414):1049–57. https://doi.org/10.1016/S0140-6736(04)15841-8 PMID: 15051286.

6. Bardeesy N, DePinho RA. Pancreatic cancer biology and genetics. Nature reviews Cancer. 2002; 2 (12):897–909. https://doi.org/10.1038/nrc949 PMID: 12459728.

7. Hidalgo M. Pancreatic cancer. The New England journal of medicine. 2010; 362(17):1605–17. https://doi.org/10.1056/NEJMra0901557 PMID: 20427809.

8. Diaferia GR, Balestrieri C, Prosperini E, Nicoli P, Spaggiari P, Zerbi A, et al. Dissection of transcriptional and cis-regulatory control of differentiation in human pancreatic cancer. The EMBO journal. 2016; 35 (6):595–617. https://doi.org/10.15252/embj.201592404 PMID: 26769127; PubMed Central PMCID: PMC4801945.

9. Kloppel G, Lingenthal G, von Bulow M, Kern HF. Histological and fine structural features of pancreatic ductal adenocarcinomas in relation to growth and prognosis: studies in xenografted tumours and clinico-histopathological correlation in a series of 75 cases. Histopathology. 1985; 9(8):841–56. https://doi.org/10.1111/j.1365-2559.1985.tb02870.x PMID: 2997015.

10. Karamitopoulou E. Role of epithelial-mesenchymal transition in pancreatic ductal adenocarcinoma: is tumor budding the missing link? Frontiers in oncology. 2013; 3:221. https://doi.org/10.3389/fonc.2013.00221 PMID: 24062980; PubMed Central PMCID: PMC3774985.

11. Arumugam T, Ramachandran V, Fournier KF, Wang H, Marquis L, Abbruzzese JL, et al. Epithelial to mesenchymal transition contributes to drug resistance in pancreatic cancer. Cancer research. 2009; 69 (14):5820–8. https://doi.org/10.1158/0008-5472.CAN-08-2819 PMID: 19584296; PubMed Central PMCID: PMC4378690.

12. Konig J, Hartel M, Nies AT, Martignoni ME, Guo J, Buchler MW, et al. Expression and localization of human multidrug resistance protein (ABCC) family members in pancreatic carcinoma. International journal of cancer. 2005; 115(3):359–67. https://doi.org/10.1002/ijc.20831 PMID: 15688370.

13. Hagmann W, Jesnowski R, Lohr JM. Interdependence of gemcitabine treatment, transporter expression, and resistance in human pancreatic carcinoma cells. Neoplasia. 2010; 12(9):740–7. https://doi.org/10.1593/neo.10576 PMID: 20824050; PubMed Central PMCID: PMC2933694.

14. Nambaru PK, Hubner T, Kock K, Mews S, Grube M, Payen L, et al. Drug efflux transporter multidrug resistance-associated protein 5 affects sensitivity of pancreatic cancer cell lines to the nucleoside anticancer drug 5-fluorouracil. Drug metabolism and disposition: the biological fate of chemicals. 2011; 39 (1):132–9. https://doi.org/10.1124/dmd.110.033613 PMID: 20930123.

15. Pratt S, Shepard RL, Kandasamy RA, Johnston PA, Perry W, Dantzig AH 3rd. The multidrug resistance protein 5 (ABCC5) confers resistance to 5-fluorouracil and transports its monophosphorylated metabolites. Molecular cancer therapeutics. 2005; 4(5):855–63. https://doi.org/10.1158/1535-7163.MCT-04-0291 PMID: 15897250.

16. Oguri T, Achiwa H, Sato S, Bessho Y, Takano Y, Miyazaki M, et al. The determinants of sensitivity and acquired resistance to gemcitabine differ in non-small cell lung cancer: a role of ABCC5 in gemcitabine sensitivity. Molecular cancer therapeutics. 2006; 5(7):1800–6. https://doi.org/10.1158/1535-7163.MCT-06-0025 PMID: 16891466.

17. Zelcer N, Saeki T, Reid G, Beijnen JH, Borst P. Characterization of drug transport by the human multidrug resistance protein 3 (ABCC3). The Journal of biological chemistry. 2001; 276(49):46400–7. https://doi.org/10.1074/jbc.M107041200 PMID: 11581266.

18. Hagmann W, Faissner R, Schnolzer M, Lohr M, Jesnowski R. Membrane drug transporters and chemoresistance in human pancreatic carcinoma. Cancers. 2010; 3(1):106–25. https://doi.org/10.3390/cancers3010106 PMID: 24212609; PubMed Central PMCID: PMC3756352.

19. Lee SH, Kim H, Hwang JH, Lee HS, Cho JY, Yoon YS, et al. Breast cancer resistance protein expression is associated with early recurrence and decreased survival in resectable pancreatic cancer patients. Pathology international. 2012; 62(3):167–75. https://doi.org/10.1111/j.1440-1827.2011.02772.x PMID: 22360504.

20. Le Large TYS, El Hassouni B, Kazemier G, Piersma SR, van Laarhoven HWM, Bijlsma MF, et al. Multi-drug-resistant transporter expression does not always result in drug resistance. Cancer science. 2018; 109(10):3360–2. https://doi.org/10.1111/cas.13756 PMID: 30195264; PubMed Central PMCID: PMC6172061.

21. Kim D, Langmead B, Salzberg SL. HISAT: a fast spliced aligner with low memory requirements. Nature methods. 2015; 12(4):357–60. https://doi.org/10.1038/nmeth.3317 PMID: 25751142; PubMed Central PMCID: PMC4655817.

22. Liao Y, Smyth GK, Shi W. featureCounts: an efficient general purpose program for assigning sequence reads to genomic features. Bioinformatics. 2014; 30(7):923–30. https://doi.org/10.1093/bioinformatics/btt656 PMID: 24227677.

23. Love MI, Huber W, Anders S. Moderated estimation of fold change and dispersion for RNA-seq data with DESeq2. Genome biology. 2014; 15(12):550. https://doi.org/10.1186/s13059-014-0550-8 PMID: 25516281; PubMed Central PMCID: PMC4302049.

24. Langmead B, Salzberg SL. Fast gapped-read alignment with Bowtie 2. Nature methods. 2012; 9 (4):357–9. https://doi.org/10.1038/nmeth.1923 PMID: 22388286; PubMed Central PMCID: PMC3322381.

25. Feng J, Liu T, Qin B, Zhang Y, Liu XS. Identifying ChIP-seq enrichment using MACS. Nature protocols. 2012; 7(9):1728–40. https://doi.org/10.1038/nprot.2012.101 PMID: 22936215; PubMed Central PMCID: PMC3868217.

26. Ramirez F, Dundar F, Diehl S, Gruning BA, Manke T. deepTools: a flexible platform for exploring deep-sequencing data. Nucleic acids research. 2014; 42(Web Server issue):W187–91. https://doi.org/10.1093/nar/gku365 PMID: 24799436; PubMed Central PMCID: PMC4086134.

27. Goecks J, Nekrutenko A, Taylor J, Galaxy T. Galaxy: a comprehensive approach for supporting accessible, reproducible, and transparent computational research in the life sciences. Genome biology. 2010; 11(8):R86. https://doi.org/10.1186/gb-2010-11-8-r86 PMID: 20738864; PubMed Central PMCID: PMC2945788.

28. Lerdrup M, Johansen JV, Agrawal-Singh S, Hansen K. An interactive environment for agile analysis and visualization of ChIP-sequencing data. Nature structural & molecular biology. 2016; 23(4):349–57. https://doi.org/10.1038/nsmb.3180 PMID: 26926434.

29. Haeussler M, Zweig AS, Tyner C, Speir ML, Rosenbloom KR, Raney BJ, et al. The UCSC Genome Browser database: 2019 update. Nucleic acids research. 2019; 47(D1):D853–D8. https://doi.org/10.1093/nar/gky1095 PMID: 30407534; PubMed Central PMCID: PMC6323953.

30. Wang S, Sun H, Ma J, Zang C, Wang C, Wang J, et al. Target analysis by integration of transcriptome and ChIP-seq data with BETA. Nature protocols. 2013; 8(12):2502–15. https://doi.org/10.1038/nprot.2013.150 PMID: 24263090; PubMed Central PMCID: PMC4135175.

31. Huang da W, Sherman BT, Lempicki RA. Bioinformatics enrichment tools: paths toward the comprehensive functional analysis of large gene lists. Nucleic acids research. 2009; 37(1):1–13. https://doi.org/10.1093/nar/gkn923 PMID: 19033363; PubMed Central PMCID: PMC2615629.

32. Ashburner M, Ball CA, Blake JA, Botstein D, Butler H, Cherry JM, et al. Gene ontology: tool for the unification of biology. The Gene Ontology Consortium. Nature genetics. 2000; 25(1):25–9. https://doi.org/10.1038/75556 PMID: 10802651; PubMed Central PMCID: PMC3037419.

33. Shannon P, Markiel A, Ozier O, Baliga NS, Wang JT, Ramage D, et al. Cytoscape: a software environment for integrated models of biomolecular interaction networks. Genome research. 2003; 13 (11):2498–504. https://doi.org/10.1101/gr.1239303 PMID: 14597658; PubMed Central PMCID: PMC403769.

34. Maere S, Heymans K, Kuiper M. BiNGO: a Cytoscape plugin to assess overrepresentation of gene ontology categories in biological networks. Bioinformatics. 2005; 21(16):3448–9. https://doi.org/10.1093/bioinformatics/bti551 PMID: 15972284.

35. Montojo J, Zuberi K, Rodriguez H, Kazi F, Wright G, Donaldson SL, et al. GeneMANIA Cytoscape plugin: fast gene function predictions on the desktop. Bioinformatics. 2010; 26(22):2927–8. https://doi.org/10.1093/bioinformatics/btq562 PMID: 20926419; PubMed Central PMCID: PMC2971582.

36. Pathan M, Keerthikumar S, Ang CS, Gangoda L, Quek CY, Williamson NA, et al. FunRich: An open access standalone functional enrichment and interaction network analysis tool. Proteomics. 2015; 15 (15):2597–601. https://doi.org/10.1002/pmic.201400515 PMID: 25921073.

37. Apweiler R, Bairoch A, Wu CH, Barker WC, Boeckmann B, Ferro S, et al. UniProt: the Universal Protein knowledgebase. Nucleic acids research. 2004; 32(Database issue):D115–9. https://doi.org/10.1093/nar/gkh131 PMID: 14681372; PubMed Central PMCID: PMC308865.

38. Bindea G, Mlecnik B, Hackl H, Charoentong P, Tosolini M, Kirilovsky A, et al. ClueGO: a Cytoscape plug-in to decipher functionally grouped gene ontology and pathway annotation networks. Bioinformatics. 2009; 25(8):1091–3. https://doi.org/10.1093/bioinformatics/btp101 PMID: 19237447; PubMed Central PMCID: PMC2666812.

39. Luo W, Pant G, Bhavnasi YK, Blanchard SG Jr., Brouwer C. Pathview Web: user friendly pathway visualization and data integration. Nucleic acids research. 2017; 45(W1):W501–W8. https://doi.org/10.1093/nar/gkx372 PMID: 28482075; PubMed Central PMCID: PMC5570256.

40. Robinson MD, McCarthy DJ, Smyth GK. edgeR: a Bioconductor package for differential expression analysis of digital gene expression data. Bioinformatics. 2010; 26(1):139–40. https://doi.org/10.1093/bioinformatics/btp616 PMID: 19910308; PubMed Central PMCID: PMC2796818.

41. Le DH, Pham VH. HGPEC: a Cytoscape app for prediction of novel disease-gene and disease-disease associations and evidence collection based on a random walk on heterogeneous network. BMC systems biology. 2017; 11(1):61. https://doi.org/10.1186/s12918-017-0437-x PMID: 28619054; PubMed Central PMCID: PMC5472867.

42. Jia N, Wang J, Li Q, Tao X, Chang K, Hua K, et al. DNA methylation promotes paired box 2 expression via myeloid zinc finger 1 in endometrial cancer. Oncotarget. 2016; 7(51):84785–97. https://doi.org/10.18632/oncotarget.12626 PMID: 27764784; PubMed Central PMCID: PMC5356698.

43. Kaku Y, Taguchi A, Tanigawa S, Haque F, Sakuma T, Yamamoto T, et al. PAX2 is dispensable for in vitro nephron formation from human induced pluripotent stem cells. Scientific reports. 2017; 7(1):4554. https://doi.org/10.1038/s41598-017-04813-3 PMID: 28674456; PubMed Central PMCID: PMC5495778.

44. Larson Gedman A, Chen Q, Kugel Desmoulin S, Ge Y, LaFiura K, Haska CL, et al. The impact of NOTCH1, FBW7 and PTEN mutations on prognosis and downstream signaling in pediatric T-cell acute lymphoblastic leukemia: a report from the Children's Oncology Group. Leukemia. 2009; 23(8):1417–25. https://doi.org/10.1038/leu.2009.64 PMID: 19340001; PubMed Central PMCID: PMC2726275.

45. Huang YK, Fan XG, Qiu F. TM4SF1 Promotes Proliferation, Invasion, and Metastasis in Human Liver Cancer Cells. International journal of molecular sciences. 2016;17(5). https://doi.org/10.3390/ijms17050661 PMID: 27153056; PubMed Central PMCID: PMC4881487.

46. Kreft L, Soete A, Hulpiau P, Botzki A, Saeys Y, De Bleser P. ConTra v3: a tool to identify transcription factor binding sites across species, update 2017. Nucleic acids research. 2017; 45(W1):W490–W4. https://doi.org/10.1093/nar/gkx376 PMID: 28472390; PubMed Central PMCID: PMC5570180.

47. Yevshin I, Sharipov R, Valeev T, Kel A, Kolpakov F. GTRD: a database of transcription factor binding sites identified by ChIP-seq experiments. Nucleic acids research. 2017; 45(D1):D61–D7. https://doi.org/10.1093/nar/gkw951 PMID: 27924024; PubMed Central PMCID: PMC5210645.

48. Pinero J, Queralt-Rosinach N, Bravo A, Deu-Pons J, Bauer-Mehren A, Baron M, et al. DisGeNET: a discovery platform for the dynamical exploration of human diseases and their genes. Database: the journal of biological databases and curation. 2015;2015:bav028. https://doi.org/10.1093/database/bav028 PMID: 25877637; PubMed Central PMCID: PMC4397996.

49. Liang WS, Craig DW, Carpten J, Borad MJ, Demeure MJ, Weiss GJ, et al. Genome-wide characterization of pancreatic adenocarcinoma patients using next generation sequencing. PloS one. 2012; 7(10): e43192. https://doi.org/10.1371/journal.pone.0043192 PMID: 23071490; PubMed Central PMCID: PMC3468610.

50. Eccles MR, Wallis LJ, Fidler AE, Spurr NK, Goodfellow PJ, Reeve AE. Expression of the PAX2 gene in human fetal kidney and Wilms' tumor. Cell growth & differentiation: the molecular biology journal of the American Association for Cancer Research. 1992; 3(5):279–89. PMID: 1378753.

51. Gokden N, Gokden M, Phan DC, McKenney JK. The utility of PAX-2 in distinguishing metastatic clear cell renal cell carcinoma from its morphologic mimics: an immunohistochemical study with comparison to renal cell carcinoma marker. The American journal of surgical pathology. 2008; 32(10):1462–7. https://doi.org/10.1097/PAS.0b013e318176dba7 PMID: 18685487.

52. Doberstein K, Pfeilschifter J, Gutwein P. The transcription factor PAX2 regulates ADAM10 expression in renal cell carcinoma. Carcinogenesis. 2011; 32(11):1713–23. https://doi.org/10.1093/carcin/bgr195 PMID: 21880579.

53. Wu H, Chen Y, Liang J, Shi B, Wu G, Zhang Y, et al. Hypomethylation-linked activation of PAX2 mediates tamoxifen-stimulated endometrial carcinogenesis. Nature. 2005; 438(7070):981–7. https://doi.org/10.1038/nature04225 PMID: 16355216.

54. Liu P, Gao Y, Huan J, Ge X, Tang Y, Shen W, et al. Upregulation of PAX2 promotes the metastasis of esophageal cancer through interleukin-5. Cellular physiology and biochemistry: international journal of experimental cellular physiology, biochemistry, and pharmacology. 2015; 35(2):740–54. https://doi.org/10.1159/000369734 PMID: 25613757.

55. Buttiglieri S, Deregibus MC, Bravo S, Cassoni P, Chiarle R, Bussolati B, et al. Role of Pax2 in apoptosis resistance and proinvasive phenotype of Kaposi's sarcoma cells. The Journal of biological chemistry. 2004; 279(6):4136–43. https://doi.org/10.1074/jbc.M306824200 PMID: 14627715.

56. Fonsato V, Buttiglieri S, Deregibus MC, Puntorieri V, Bussolati B, Camussi G. Expression of Pax2 in human renal tumor-derived endothelial cells sustains apoptosis resistance and angiogenesis. The American journal of pathology. 2006; 168(2):706–13. https://doi.org/10.2353/ajpath.2006.050776 PMID: 16436683; PubMed Central PMCID: PMC1606486.

57. Cao J, Ma J, Sun L, Li J, Qin T, Zhou C, et al. Targeting glypican-4 overcomes 5-FU resistance and attenuates stem cell-like properties via suppression of Wnt/beta-catenin pathway in pancreatic cancer cells. Journal of cellular biochemistry. 2018; 119(11):9498–512. https://doi.org/10.1002/jcb.27266 PMID: 30010221.

58. Wang W, Zhao L, Wei X, Wang L, Liu S, Yang Y, et al. MicroRNA-320a promotes 5-FU resistance in human pancreatic cancer cells. Scientific reports. 2016; 6:27641. https://doi.org/10.1038/srep27641 PMID: 27279541; PubMed Central PMCID: PMC4899709.

59. Sun FX, Tohgo A, Bouvet M, Yagi S, Nassirpour R, Moossa AR, et al. Efficacy of camptothecin analog DX-8951f (Exatecan Mesylate) on human pancreatic cancer in an orthotopic metastatic model. Cancer research. 2003; 63(1):80–5. PMID: 12517781.

60. Stathopoulos GP, Rigatos SK, Dimopoulos MA, Giannakakis T, Foutzilas G, Kouroussis C, et al. Treatment of pancreatic cancer with a combination of irinotecan (CPT-11) and gemcitabine: a multicenter phase II study by the Greek Cooperative Group for Pancreatic Cancer. Annals of oncology: official journal of the European Society for Medical Oncology. 2003; 14(3):388–94. https://doi.org/10.1093/annonc/mdg109 PMID: 12598343.

61. Jeansonne DP, Koh GY, Zhang F, Kirk-Ballard H, Wolff L, Liu D, et al. Paclitaxel-induced apoptosis is blocked by camptothecin in human breast and pancreatic cancer cells. Oncology reports. 2011; 25(5):1473–80. https://doi.org/10.3892/or.2011.1187 PMID: 21331447.

62. Fueger BJ, Hamilton G, Raderer M, Pangerl T, Traub T, Angelberger P, et al. Effects of chemotherapeutic agents on expression of somatostatin receptors in pancreatic tumor cells. Journal of nuclear medicine: official publication, Society of Nuclear Medicine. 2001; 42(12):1856–62. PMID: 11752085.

63. Halloran CM, Ghaneh P, Shore S, Greenhalf W, Zumstein L, Wilson D, et al. 5-Fluorouracil or gemcitabine combined with adenoviral-mediated reintroduction of p16INK4A greatly enhanced cytotoxicity in Panc-1 pancreatic adenocarcinoma cells. The journal of gene medicine. 2004; 6(5):514–25. https://doi.org/10.1002/jgm.540 PMID: 15133762.

64. Wang WB, Yang Y, Zhao YP, Zhang TP, Liao Q, Shu H. Recent studies of 5-fluorouracil resistance in pancreatic cancer. World journal of gastroenterology. 2014; 20(42):15682–90. https://doi.org/10.3748/wjg.v20.i42.15682 PMID: 25400452; PubMed Central PMCID: PMC4229533.

65. Neoptolemos JP, Stocken DD, Bassi C, Ghaneh P, Cunningham D, Goldstein D, et al. Adjuvant chemotherapy with fluorouracil plus folinic acid vs gemcitabine following pancreatic cancer resection: a randomized controlled trial. Jama. 2010; 304(10):1073–81. https://doi.org/10.1001/jama.2010.1275 PMID: 20823433.

66. Damaraju VL, Damaraju S, Young JD, Baldwin SA, Mackey J, Sawyer MB, et al. Nucleoside anticancer drugs: the role of nucleoside transporters in resistance to cancer chemotherapy. Oncogene. 2003; 22(47):7524–36. https://doi.org/10.1038/sj.onc.1206952 PMID: 14576856.

67. Duxbury MS, Ito H, Zinner MJ, Ashley SW, Whang EE. Inhibition of SRC tyrosine kinase impairs inherent and acquired gemcitabine resistance in human pancreatic adenocarcinoma cells. Clinical cancer research: an official journal of the American Association for Cancer Research. 2004; 10(7):2307–18. PMID: 15073106.

68. Liau SS, Whang E. HMGA1 is a molecular determinant of chemoresistance to gemcitabine in pancreatic adenocarcinoma. Clinical cancer research: an official journal of the American Association for Cancer Research. 2008; 14(5):1470–7. https://doi.org/10.1158/1078-0432.CCR-07-1450 PMID: 18316571; PubMed Central PMCID: PMC2652398.

69. Farrell JJ, Bae K, Wong J, Guha C, Dicker AP, Elsaleh H. Cytidine deaminase single-nucleotide polymorphism is predictive of toxicity from gemcitabine in patients with pancreatic cancer: RTOG 9704. The

pharmacogenomics journal. 2012; 12(5):395–403. https://doi.org/10.1038/tpj.2011.22 PMID: 21625252.

70. Nath S, Daneshvar K, Roy LD, Grover P, Kidiyoor A, Mosley L, et al. MUC1 induces drug resistance in pancreatic cancer cells via upregulation of multidrug resistance genes. Oncogenesis. 2013; 2:e51. https://doi.org/10.1038/oncsis.2013.16 PMID: 23774063; PubMed Central PMCID: PMC3740301.

71. Zhang W, Chen H, Liu DL, Li H, Luo J, Zhang JH, et al. Emodin sensitizes the gemcitabine-resistant cell line Bxpc-3/Gem to gemcitabine via downregulation of NF-kappaB and its regulated targets. International journal of oncology. 2013; 42(4):1189–96. https://doi.org/10.3892/ijo.2013.1839 PMID: 23440366.

72. Aguirre-Gamboa R, Gomez-Rueda H, Martinez-Ledesma E, Martinez-Torteya A, Chacolla-Huaringa R, Rodriguez-Barrientos A, et al. SurvExpress: an online biomarker validation tool and database for cancer gene expression data using survival analysis. PloS one. 2013; 8(9):e74250. https://doi.org/10.1371/journal.pone.0074250 PMID: 24066126; PubMed Central PMCID: PMC3774754.

73. Stratford JK, Bentrem DJ, Anderson JM, Fan C, Volmar KA, Marron JS, et al. A six-gene signature predicts survival of patients with localized pancreatic ductal adenocarcinoma. PLoS medicine. 2010; 7(7): e1000307. https://doi.org/10.1371/journal.pmed.1000307 PMID: 20644708; PubMed Central PMCID: PMC2903589.

74. Zhang G, Schetter A, He P, Funamizu N, Gaedcke J, Ghadimi BM, et al. DPEP1 inhibits tumor cell invasiveness, enhances chemosensitivity and predicts clinical outcome in pancreatic ductal adenocarcinoma. PloS one. 2012; 7(2):e31507. https://doi.org/10.1371/journal.pone.0031507 PMID: 22363658; PubMed Central PMCID: PMC3282755.

75. Zhang G, He P, Tan H, Budhu A, Gaedcke J, Ghadimi BM, et al. Integration of metabolomics and transcriptomics revealed a fatty acid network exerting growth inhibitory effects in human pancreatic cancer. Clinical cancer research: an official journal of the American Association for Cancer Research. 2013; 19 (18):4983–93. https://doi.org/10.1158/1078-0432.CCR-13-0209 PMID: 23918603; PubMed Central PMCID: PMC3778077.

76. Swayden M, Iovanna J, Soubeyran P. Pancreatic cancer chemo-resistance is driven by tumor phenotype rather than tumor genotype. Heliyon. 2018; 4(12):e01055. https://doi.org/10.1016/j.heliyon.2018.e01055 PMID: 30582059; PubMed Central PMCID: PMC6299038.

77. Mezencev R, Matyunina LV, Wagner GT, McDonald JF. Acquired resistance of pancreatic cancer cells to cisplatin is multifactorial with cell context-dependent involvement of resistance genes. Cancer gene therapy. 2016; 23(12):446–53. https://doi.org/10.1038/cgt.2016.71 PMID: 27910856; PubMed Central PMCID: PMC5159445.

78. Gnanamony M, Gondi CS. Chemoresistance in pancreatic cancer: Emerging concepts. Oncology letters. 2017; 13(4):2507–13. https://doi.org/10.3892/ol.2017.5777 PMID: 28454427; PubMed Central PMCID: PMC5403303.

79. Grasso C, Jansen G, Giovannetti E. Drug resistance in pancreatic cancer: Impact of altered energy metabolism. Critical reviews in oncology/hematology. 2017; 114:139–52. https://doi.org/10.1016/j.critrevonc.2017.03.026 PMID: 28477742.

80. Gaianigo N, Melisi D, Carbone C. EMT and Treatment Resistance in Pancreatic Cancer. Cancers. 2017;9(9). https://doi.org/10.3390/cancers9090122 PMID: 28895920; PubMed Central PMCID: PMC5615337.

81. Andor N, Graham TA, Jansen M, Xia LC, Aktipis CA, Petritsch C, et al. Pan-cancer analysis of the extent and consequences of intratumor heterogeneity. Nature medicine. 2016; 22(1):105–13. https://doi.org/10.1038/nm.3984 PMID: 26618723; PubMed Central PMCID: PMC4830693.

82. Hagmann W, Jesnowski R, Faissner R, Guo C, Lohr JM. ATP-binding cassette C transporters in human pancreatic carcinoma cell lines. Upregulation in 5-fluorouracil-resistant cells. Pancreatology: official journal of the International Association of Pancreatology. 2009; 9(1–2):136–44. https://doi.org/10.1159/000178884 PMID: 19077464.

83. Cao J, Yang J, Ramachandran V, Arumugam T, Deng D, Li Z, et al. TM4SF1 Promotes Gemcitabine Resistance of Pancreatic Cancer In Vitro and In Vivo. PloS one. 2015; 10(12):e0144969. https://doi.org/10.1371/journal.pone.0144969 PMID: 26709920; PubMed Central PMCID: PMC4692438.

84. Ireland L, Santos A, Ahmed MS, Rainer C, Nielsen SR, Quaranta V, et al. Chemoresistance in Pancreatic Cancer Is Driven by Stroma-Derived Insulin-Like Growth Factors. Cancer research. 2016; 76 (23):6851–63. https://doi.org/10.1158/0008-5472.CAN-16-1201 PMID: 27742686; PubMed Central PMCID: PMC5321488.

85. Ueda T, Ito S, Shiraishi T, Taniguchi H, Kayukawa N, Nakanishi H, et al. PAX2 promoted prostate cancer cell invasion through transcriptional regulation of HGF in an in vitro model. Biochimica et biophysica acta. 2015; 1852(11):2467–73. https://doi.org/10.1016/j.bbadis.2015.08.008 PMID: 26296757.

86. Song H, Kwan SY, Izaguirre DI, Zu Z, Tsang YT, Tung CS, et al. PAX2 Expression in Ovarian Cancer. International journal of molecular sciences. 2013; 14(3):6090–105. https://doi.org/10.3390/ijms14036090 PMID: 23502471; PubMed Central PMCID: PMC3634442.

87. Silberstein GB, Dressler GR, Van Horn K. Expression of the PAX2 oncogene in human breast cancer and its role in progesterone-dependent mammary growth. Oncogene. 2002; 21(7):1009–16. https://doi.org/10.1038/sj.onc.1205172 PMID: 11850818.

88. Aslan M, Shahbazi R, Ulubayram K, Ozpolat B. Targeted Therapies for Pancreatic Cancer and Hurdles Ahead. Anticancer research. 2018; 38(12):6591–606. https://doi.org/10.21873/anticanres.13026 PMID: 30504367.

89. Chand S, O'Hayer K, Blanco FF, Winter JM, Brody JR. The Landscape of Pancreatic Cancer Therapeutic Resistance Mechanisms. International journal of biological sciences. 2016; 12(3):273–82. https://doi.org/10.7150/ijbs.14951 PMID: 26929734; PubMed Central PMCID: PMC4753156.

90. Bhagwandin VJ, Bishop JM, Wright WE, Shay JW. The Metastatic Potential and Chemoresistance of Human Pancreatic Cancer Stem Cells. PloS one. 2016; 11(2):e0148807. https://doi.org/10.1371/journal.pone.0148807 PMID: 26859746; PubMed Central PMCID: PMC4747523.